

Intercalibration of the Infrared Channels between GMS-5 and GOES-9

TAHARA Yoshihiko*, OHKAWARA Nozomu*, and OKUYAMA Arata*

Abstract

This study investigates intercalibration between the GOES-9 Imager and GMS-5 VISSR infrared channels. Observed and simulated brightness temperatures from GOES-9 and GMS-5 are used for this purpose. The observed brightness temperatures are obtained from images observed just before the switchover from GMS-5 to GOES-9; the simulated brightness temperatures are computed by MODTRAN 3.7. In the comparison of the horizontal images, a difference between GOES-9 and GMS-5 is recognized, as expected from their spectral response functions and each radiative path. Further, as the result of the statistical comparison of observed brightness temperatures with the same radiative path length from the satellites within the cloud-free ocean area, discrepancies inconsistent with simulations are detected. The averages of the discrepancies between GOES-9 and GMS-5 with respect to residuals of the observed from simulated brightness temperatures are 0.7 K for the infrared window channel 1 (IR1), 0.28 K for the infrared window channel 2 (IR2) and 2.4 K for the water vapor channel (WV). Potential sources of the differences are inaccurate calibration, the unveiled degradation of the sensors and the satellites, systematic error in the simulated brightness temperatures, etc. In order to identify the source, further research is necessary. Despite the fact that the sources are unconfirmed, the result of this study may be of help to revise the algorithms of GOES-9 applications. For instance, a linear relationship is found between GOES-9 and GMS-5 with respect to difference between the IR1 and IR2 brightness temperatures.

1. Introduction

The Geostationary Meteorological Satellite 5 (GMS-5) was launched on 18 March 1995, carrying the Visible and Infrared Spin Scan Radiometer (VISSR) to provide cloud and water vapor images over the west Pacific region. Its observation had lasted for 8 years, exceeding the designed lifetime of 5 years. Due to the shortage of fuel for satellite orbital control and the degradation of the mirror controller in VISSR, the Geostationary Operational Environmental Satellite 9 (GOES-9) started its operational observation over the west Pacific region on 22 May 2003, substituting for GMS-5. GOES-9 also carries an imager, called the

GOES-9 Imager, providing cloud and water vapor images successively.

Figure 1 shows the examples of infrared images observed by (a) the GOES-9 Imager and (b) the GMS-5 VISSR at the same time. The two images provide the similar information about cloud and weather systems, except for the 15-longitude-degree difference in the observed region. The information is important for not only weather and climate watch, but also generating physical parameters, such as atmospheric wind vectors, aerosol, volcanic ash and sea ice, etc. Therefore, it is important to survey the

*System Engineering Division, Meteorological Satellite Center
Received December 2, 2003. Revised February 17, 2004.

differences in the images between GOES-9 Imager and GMS-5 VISSR in order to maintain the accuracy of the products. This paper reports the results of comparisons between images simultaneously observed just before the switchover from GMS-5 to GOES-9. In the GOES-9 images of GVAR data, some noise is contained as shown in Figure 2. The noise is also noted at the end of this paper.

2. Comparison of Specifications

GMS-5 flies in a geosynchronous orbit at 140 E. VISSR aboard GMS-5 has four channels; two channels are in the infrared window region (IR1 and IR2); the other two channels are in the infrared water vapor region (WV) and the visible region (VIS). Table 1 shows the spectral bands and the spatial resolutions of these channels. The details of calibration for GMS-5 VISSR are found in MSC, 1997, Tokuno et al, 1997, and Kurihara et al, 2000.

GOES-9 has been placed in a geosynchronous orbit at 155 E since 25 April 2003. Its operational observation at the longitude started on 22 May. The imager aboard GOES-9 has five channels; four of them have similar spectral bands to VISSR, and one additional channel is in the short wave infrared window region (SWIR). The spectral bands and the resolutions of these channels are shown in Table 1 as well as IR1. The details of calibration for GOES-9 Imager are found in 'GOES Data Book' by NASA, 2001, and the web pages of NASA and NESDIS on the Internet. To avoid confusion caused by resemblance between the sensor name GOES "Imager" and the sensor's category name "imager," simply the satellite name is used to denote the onboard sensor hereafter.

Figure 3 shows the spectral response functions of the infrared channels of (a) GOES-9 and (b) GMS-5 as a function of wavenumber. IR2 is located in a smaller wavenumber region than IR1 for both GOES-9 and GMS-5. GOES-9 IR1 and GMS-5 IR1 are approximately in the same spectral region with each other, while GOES-9 IR2 is in a smaller

wavenumber region than GMS-5 IR2. Water vapor continuum is the major source of absorption for IR1 and IR2. The absorption becomes larger as the wavenumber is smaller. Hence, IR2 is more affected by the absorption than IR1, and GOES-9 IR2 is more affected than GMS-5 IR2. The WV channels of GOES-9 and GMS-5 are in the spectral region of strong absorption by water vapor transition. Since GOES-9 WV is in a larger wavenumber region than GMS-5 WV, GOES-9 WV is more affected by the absorption than GMS-5 WV. The large absorption, consequently less transparent, makes the brightness temperature low. Therefore, the IR2 brightness temperatures of both GOES-9 and GMS-5 are expected to be lower than the corresponding IR1 brightness temperatures. Similarly, the brightness temperatures of both GOES-9 IR2 and WV are lower than the corresponding GMS-5 brightness temperatures.

Figure 4 shows the spectral response functions of GOES-9 VIS (thin lines) and GMS-5 VIS (thick line) as a function of wavelength. The spectral band of GOES-9 VIS is narrower than that of GMS-5 VIS. That may affect some products using the VIS channel, such as volcanic ash and aerosol. However, the VIS channels aren't compared in this study, since the geosynchronous orbital difference between GOES-9 and GMS-5 makes the comparison difficult. A polar-orbiting satellite is necessary for the intercalibration of VIS.

The difference in the geosynchronous orbits makes a difference in the radiative path through the atmosphere from the earth surface to the two satellites. Assuming the atmosphere is plain parallel and homogeneous at each observing point, the difference in the radiative paths is equivalent to the difference in the path length. A longer radiative path makes atmospheric absorption and scattering effects larger. Figure 5 shows the secants of the satellite zenith angles of GOES-9 (a) and GMS-5 (b), which are approximately proportional to the path lengths. Figure 5 (c) shows the difference between Figures (a) and (b). The lengths

from the longitude line at 147.5 E to the two satellites are equal. A length from the surface to GOES-9 is longer than that to GMS-5 on the west side of 147.5 E, and vice versa on the east side.

3. Comparison of Images

Figures 6 (a) and (b) show the images of IR1 brightness temperatures of 06 UTC 19 May 2003, as observed by GOES-9 (a) and GMS-5 (b). Figure (c) shows the differences computed by subtracting the temperatures of Figure (b) from those of Figure (a). Figure (d) shows the same as Figure (c), but for brightness temperatures simulated by the Moderate Resolution Model for LOWTRAN 7 (MODTRAN 3.7) (Berk et al, 1989). In the simulation, any atmospheric scattering is neglected.

Atmospheric absorption is estimated by using the three-dimensional grid data of the atmospheric fields forecasted by the global numerical weather prediction model of the Japan Meteorological Agency. The data is interpolated to 1.25-degree grids with 16 vertical levels up to 10 hPa. The simulation is performed only over the ocean, while surface emissivity is assumed to be invariably 0.98.

It is impossible to recognize a distinct difference between the GOES-9 image in Figure (a) and the GMS-5 one in Figure (b). However, Figure (c) indicates that the difference between the images has a zonal trend. The simulated difference shown in Figure (d) also represents the same trend. The trend is caused in association with the difference in radiative path lengths to the two satellites. Regarding the clear sky and low cloud areas colored in red and orange in Figures (a) and (b), the zonal trend in Figures (c) is approximately the same with the zonal trend in Figure (d). Over the thin cloud and wet atmosphere areas drawn in light blue and green in Figures (a) and (b), the zonal trend in Figure (c) is enhanced. Regarding the thick cloud areas colored in dark blue in Figures (a) and (b), the differences between the satellites in Figure (c) are

small and drawn in green, particularly over SPCZ and ITCZ. The differences are negative over the Bay of Bengal and the South China Sea, even though dark blue points are observed there in Figures (a) and (b). The feature is not recognized consistently over SPCZ and ITCZ. The reason is that only upper thin cloud covers are observed over the Bay of Bengal and the South China Sea at the time.

Figure 7 shows the same comparisons as Fig. 6, but for IR2 images. Similar to IR1, no distinct difference can be recognized in the observed images between Figures (a) and (b). A zonal trend similar to IR1 is seen in Figures (c) and (d). Comparing Figures 6 (c) and 7 (c) over the clear sky area, the IR2 brightness temperature residuals of GOES-9 from GMS-5 are lower than the IR1 residuals. The similar feature is recognized in the simulated images between Figures 6 (d) and 7 (d). In terms of the relation to the cloudy areas, the same discussion can be conducted as for IR1; there is a large zonal trend over the thin cloud, but small differences over the thick cloud.

Figure 8 shows the same comparisons as Fig. 6, but for differences in brightness temperatures between the split window channels, $\delta T_{SP} = T_{IR1} - T_{IR2}$. The positive temperature differences of GOES-9 dominate over the Tropics as shown in Figure (a) due to the difference in the water vapor absorption between IR1 and IR2. The temperature differences decrease in the mid-latitude, where moisture in the atmosphere is less than one in the Tropics. The temperature differences are neutral over the cloud. The GMS-5 image in Figure (b) shows similar features to GOES-9. However, the temperature differences of GMS-5 are smaller than those of GOES-9, since the difference in the spectral response functions between GMS-5 IR1 and IR2 is small. Figures (c) and (d) do not show a clear zonal trend. This denotes that the differences between GOES-9 and GMS-5 of the temperature differences are zero or negatively correlated with path lengths.

Figure 9 shows the same comparisons as Fig. 6, but for WV images. The brightness temperatures of GOES-9 in Figure (a) are lower than those of GMS-5 in Figure (b), since GOES-9 WV is less transparent than GMS-5 WV. The observed differences between GOES-9 and GMS-5 in Figure (c) are less than the simulated differences in Figure (d). This inconsistency will be discussed in the next section.

4. Comparison of Statistics

The differences between the image data of GOES-9 and GMS-5 shown in Figures 6 to 9 are originated in the characteristics of the sensors and the radiative paths. In order to survey the difference associated with the sensors, the brightness temperatures are compared statistically. The method of the comparison is referred to Gunshor et al (2001). The region for the comparison is from 140 E to 155 E and from 45 S to 45 N, where radiative path lengths from the earth surface to the two satellites are approximately the same. The observational times of the data used in this study are at 00, 06, 12 and 18 UTC on 19 May 2003. In order to match up the observations between GOES-9 and GMS-5, the brightness temperatures are averaged in 0.25 latitude and longitude degree boxes. The averaged temperatures, whose box domains are entirely over the ocean and cloud free, are applied only to the statistical computation. For the elimination of the cloudy data, the technique of cloud detection used in the SST retrieval (Yasuda and Shirakawa, 1999) is applied. The brightness temperatures simulated by MODTRAN 3.7 are also evaluated. Matching up the brightness temperatures between the observations and the simulations and also between GOES-9 and GMS-5, 68 sets of the brightness temperatures are obtained.

Figure 10 shows the comparisons of the IR1 brightness temperatures. Figure (a) shows a comparison between the observed and the simulated temperatures of GOES-9, and Figure (b) shows the same comparison but GMS-5. Figure (c) shows a comparison between GOES-9 and GMS-5 of the

observed temperatures, and Figure (d) shows the same comparison but the simulated temperatures. Points in Figures (c) and (d) are located along with the diagonal lines, while the points are spread across the lines in Figures (a) and (b). This suggests that the diffusion of the points is generated by systematic error in the simulated brightness temperatures. The diffusive error originates mainly from inaccuracy in the water vapor and sea surface temperature fields computed by the numerical weather prediction system and incorrectness in the water vapor absorption estimated by MODTRAN.

The observed brightness temperatures of GOES-9 are higher than those of GMS-5, as recognized in Figure (c). On the other hand, the simulated brightness temperatures of GOES-9 are less biased than those of GMS-5 in Figure (d), as expected by the similarity of the spectral bands between GOES-9 IR1 and GMS-5 IR1. Therefore, the difference in the spectral response functions cannot explain the discrepancy recognized in Figure (c). Figure (e) shows a comparison between GOES-9 and GMS-5 with respect to the residuals of the observed brightness temperatures from the simulated temperatures. Figure (f) shows a comparison between observation and simulation with respect to the residuals of the GOES-9 brightness temperatures from the GMS-5 temperatures. The departures of the points from the diagonal lines in Figures (e) and (f) represent discrepancies in the observations between GOES-9 and GMS-5 unpredicted by the simulation. The average of the unpredictable discrepancies,

$$\begin{aligned} & \overline{\delta T}_{\text{IR1, obs-cal}}^{\text{GOES9-GMS5}} \\ & = \langle (T_{\text{IR1, obs}}^{\text{GOES9}} - T_{\text{IR1, cal}}^{\text{GOES9}}) - (T_{\text{IR1, obs}}^{\text{GMS5}} - T_{\text{IR1, cal}}^{\text{GMS5}}) \rangle, \end{aligned}$$

is +0.70 K.

Figure 11 shows the same comparisons as Fig. 10, except for IR2 brightness temperatures. Diffusion similar to Figures 10 (a) and (b) can be recognized in Figures 11 (a) and (b) respectively. The diffusion in Fig. 11 (a) is slightly larger than that in Figure (b), since the water vapor absorption of

GOES-9 IR2 is larger than that of GMS-5 IR2 and increases its estimation error. As shown in Figures (c) and (d), the brightness temperatures of GOES-9 are smaller than those of GMS-5, which is expected in Section 2. As well as IR1, there are the discrepancies in the IR2 observed brightness temperatures between GOES-9 and GMS-5, which are not predicted by the simulation. The average of the unpredictable discrepancies, $\overline{\delta T}_{IR2, obs-cal}^{GOES9-GMS5}$, is +0.28 K.

Figure 12 shows the same comparisons as Fig. 10, except for the brightness temperature differences of IR1 from IR2, $\delta T_{SP} = T_{IR1} - T_{IR2}$. As shown in Fig. 12 (c), the observed the temperature differences of GOES-9 are larger than those of GMS-5. The fact is expected from the discussion about the spectral response functions in Section 2 and simulated in Figure (d). However, inconsistency is recognized between Figures (c) and (d). The average of the discrepancies in the observations between GOES-9 and GMS-5 unpredicted by the simulation, $\overline{\delta T}_{SP, obs-cal}^{GOES9-GMS5}$, is +0.42 K. As seen in Figures (c) and (d), the temperature differences have a linear relationship between GOES-9 and GMS-5 given by

$$\delta T_{SP, obs}^{GOES9} = 2.09\delta T_{SP, obs}^{GMS5} + 0.65 \quad (\text{Fig. (c)}), \quad (1)$$

$$\delta T_{SP, cal}^{GOES9} = 1.77\delta T_{SP, cal}^{GMS5} + 0.28 \quad (\text{Fig. (d)}), \quad (2)$$

respectively. These equations may be of help to transform a GMS-5 product to a GOES-9 one, which uses the temperature differences in its retrieval.

Figure 13 shows the same comparisons as Fig. 10, except for WV brightness temperatures. The points in Figures 13 (a) and (b) are spread wider than those seen in Fig. 6 for IR1 and Fig. 7 for IR2. Erroneousness in the estimation of the large water vapor absorption is enhanced. Many points in Figure (b) are positioned around the diagonal line, while the plots are above the diagonal line in Figure (a). However, the fact does not denote that the GMS-5 observations are more accurate than

the GOES-9 observations, because the brightness temperature simulation could have the same systematical error as the GMS-5 observations have. Figures (c) and (d) show that the brightness temperatures of GOES-9 are smaller than those of GMS-5, since the water vapor absorption for GOES-9 is larger than that for GMS-5. The averaged difference in the observed brightness temperatures of GOES-9 from GMS-5 is -5.17 K, while the averaged difference in the simulated temperatures is -7.60 K. The inconsistencies between the observations and the simulations are obviously recognized in the horizontal images shown in Figures 9 (c) and (d). As well as IR1 and IR2, there are the discrepancies between the GOES-9 and GMS-5 WV observed brightness temperatures that are not predicted by the simulation. The average of the unpredictable discrepancies, $\overline{\delta T}_{WV, obs-cal}^{GOES9-GMS5}$, is +2.4 K.

5. Conclusion

The infrared images simultaneously observed by the GOES-9 Imager and GMS-5 VISSR are compared. In addition, the simulated images computed by MODTRAN 3.7 are compared. The differences between GOES-9 and GMS-5 are observed as expected from their spectral response functions and each radiative path. The distinct inconsistencies are also recognized between the observed and simulated WV images.

Statistical comparison is also studied. Brightness temperatures from the images are compared over the cloud free ocean and the same path lengths. The differences between the GOES-9 and GMS-5 observed brightness temperatures are recognized. The differences are not equivalent to those in the simulated brightness temperatures not only for WV, but also for IR1 and IR2. The averages of the discrepancies in the observed brightness temperatures between GOES-9 and GMS-5 not predicted by the simulation, $\overline{\delta T}_{obs-cal}^{GOES9-GMS5}$, are +0.70 K, +0.28 K and +2.4 K for IR1, IR2 and WV respectively.

The potential sources of the discrepancies are inaccurate

calibration, unveiled degradation in the sensors and satellites, the retrieval error of the spectral response functions, and systematic error in the brightness temperatures simulated by MODTRAN 3.7 and atmospheric fields computed by the numerical weather prediction model, etc. In order to identify the sources, further research is necessary.

Despite the fact that the sources are not confirmed, the discussion in Sections 3 and 4 may be of help to revise the algorithms of GOES-9 applications. For instance, a linear relationship is found between GOES-9 and GMS-5 with respect to the difference between IR1 and IR2 brightness temperatures.

6. Notes

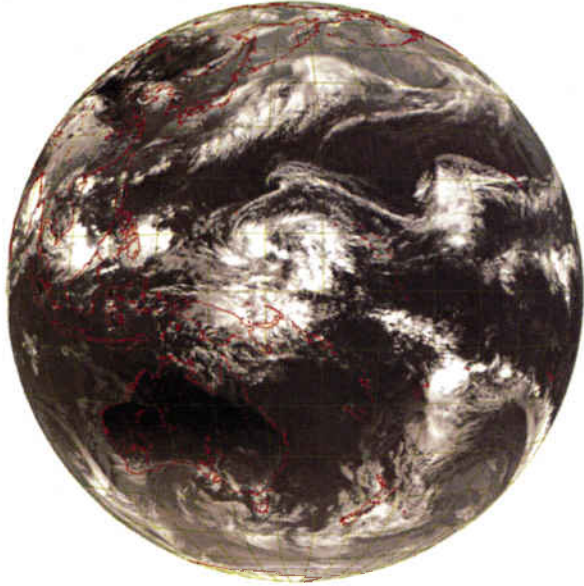
Some noise is recognized in the GOES-9 images contained in GVAR data generated by NESDIS. Figure 2 (a) shows an enlarged image observed by GOES-9 VIS. Anomalous noise can be recognized. In order to eliminate it, a digital filtering technique, which consists of a band pass filter with an amplitude limitation, is applied at the Meteorological Satellite Center. The details of the noise reduction technique can be found in Kigawa et al, 2002.

Stripe noise associated with scan lines can also be observed in GOES-9 IR1 and IR2 images contained in GVAR data. The noise is recognized only in the range of brightness temperature higher than 293 K, even though the temperature should be homogeneous over the cloud free ocean. The variation of the noise is approximately 0.5 K for IR2 and 0.2 K for IR1. The noise is negligible for observing weather systems from GOES-9 images. However, it may not be negligible to retrieve physical quantities. For instance, the influence of the noise is emphasized in the difference between IR1 and IR2 brightness temperatures as shown in Fig. 2 (b). The noise may cause the degradation of some products. In order to eliminate the stripe noise, further research is needed as well.

References

- Berk, A., L. S. Bernstein and D. C. Roberson, 1989: MODTRAN: A Moderate Resolution Model for LOWTRAN 7. GL-TR-89-0122.
- Gunshor, M. M., T. J. Schmit and W. P. Menzel, 2001: Intercalibration of geostationary and polar orbiting infrared window and water vapor radiances. Extended Abstracts, Eleventh Conf. on Satellite Meteorology and Oceanography, Madison, Wisconsin, Amer. Meteor. Soc., 438-441.
- Kigawa, S., and D. Chesters, 2002: Digital Noise Filter for GOES-9 Visible Channel. Meteorological Satellite Center Technical Note, No. 41, 21-35.
- Kurihara, S., and M. Tokuno, 2000: The Status of Calibration of VISSR on board GMS-5. Meteorological Satellite Center Technical Note, No. 38, 53-68. (written in Japanese)
- Meteorological Satellite Center, 1997: The GMS User's Guide Third Edition.
- NASA, 2001: GOES Data Book.
- Tokuno, M., H. Itaya, K. Tsuchiya and S. Kurihara, 1997: Calibration of VISSR Onboard GMS-5. Adv. Space Res., 19, 9, 1297-1306.
- Yasuda, Hiroaki, and Yoshishige Shirakawa, 1999: Improvement of the Derivation Method of Sea Surface Temperature from GMS-5 Data. Meteorological Satellite Center Technical Note, No. 37, 19-33. (written in Japanese)
- NASA: 'GOES Project Science by NASA'.
<http://rsd.gsfc.nasa.gov/goes/>
- NOAA/NESDIS: 'Geostationary Operational Environmental Satellites'.
<http://www.oso.noaa.gov/goes/>

(a) GOES-9 Imager IR1



(b) GMS-5 VISSR IR1

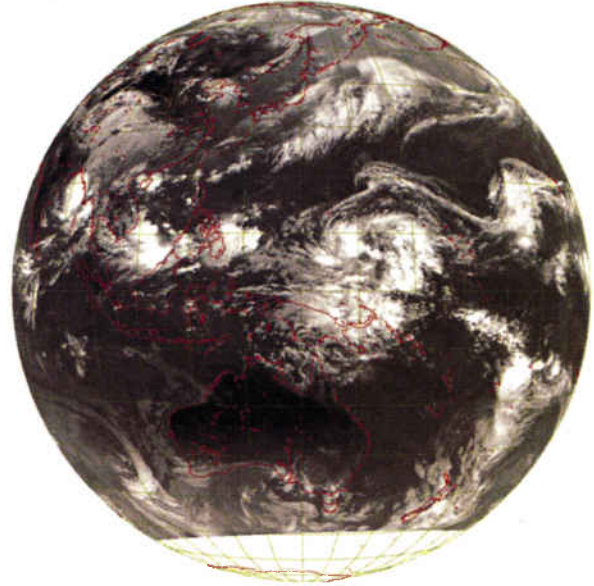
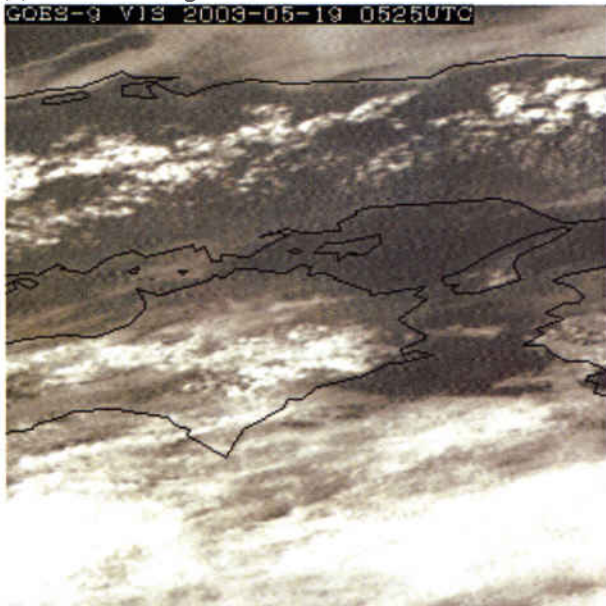


Figure 1: Cloud images observed by the IR1 channels of GOES-9 Imager (a) and GMS-5 VISSR (b) at 06 UTC on 19 May 2003.

(a) GOES-9 Imager VIS



(b) GOES-9 Imager IR1 minus IR2

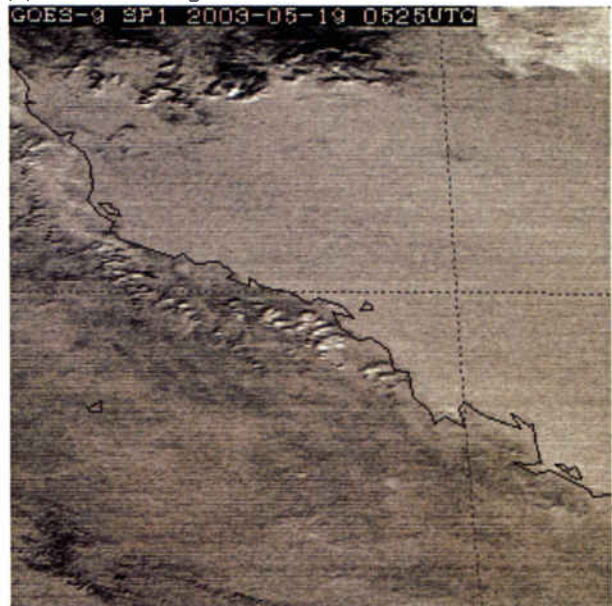


Figure 2: Images observed by GOES-9 Imager of (a) the VIS channel over western Japan and (b) the difference in the brightness temperatures between GOES-9 IR1 and IR2 over north east Australia. The observational time is the same as Figure 1.

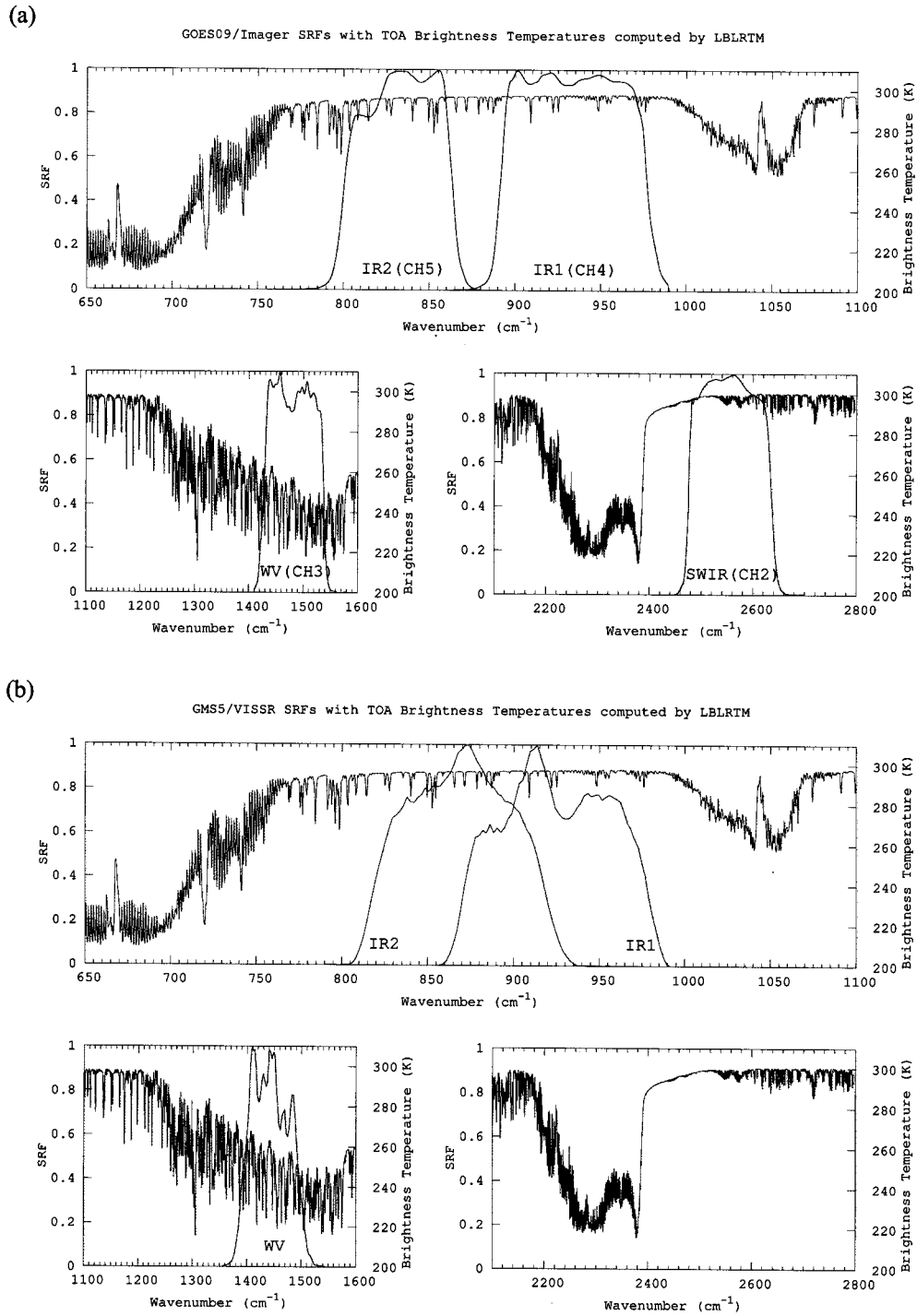


Figure 3: Spectral response functions of the infrared channels of GOES-9 Imager (a) and GMS-5 VISSR (b) as a function of wavenumber. The thin line represents the brightness temperatures of out-going radiances from the top of the atmosphere computed by LBLRTM using the U.S. standard atmosphere.

Table 1: Comparison of specifications between GOES-9 Imager and GMS-5 VISSR. The resolutions represent footprint sizes near nadir.

Satellite/Sensor	GOES-9/Imager		GMS-5/VISSR	
Geosynchronous position	155°E		140°E	
Channels	Wavelength	(Res.)	Wavelength	(Res.)
VIS (Visible)	0.55 – 0.75 μm	(1 km)	0.55 – 0.9 μm	(1.25 km)
IR1 (IR Window 1)	10.2 – 11.2 μm	(4 km)	10.5 – 11.5 μm	(5 km)
IR2 (IR Window 2)	11.5 – 12.5 μm	(4 km)	11.5 – 12.5 μm	(5 km)
WV (Water Vapor)	6.5 – 7.0 μm	(8 km)	6.5 – 7.0 μm	(5 km)
SWIR (Short Wave IR)	3.8 – 4.0 μm	(4 km)	(NA)	(NA)

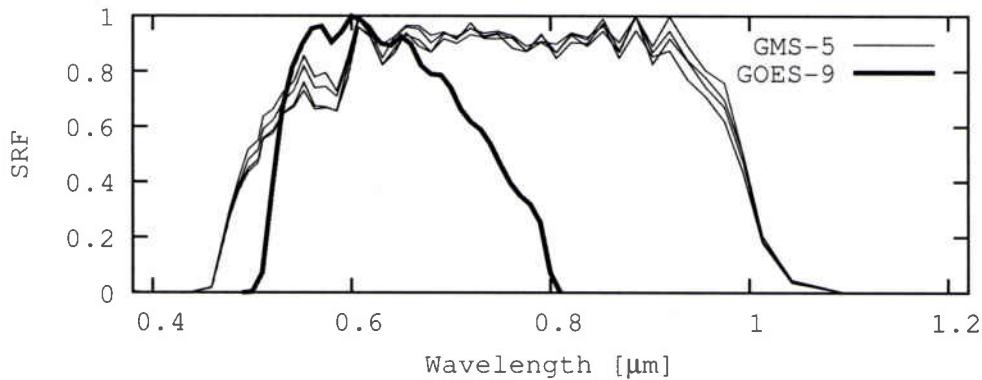


Figure 4: Spectral response functions of the visible channels of GOES-9 Imager (thin lines) and GMS-5 VISSR (thick line).

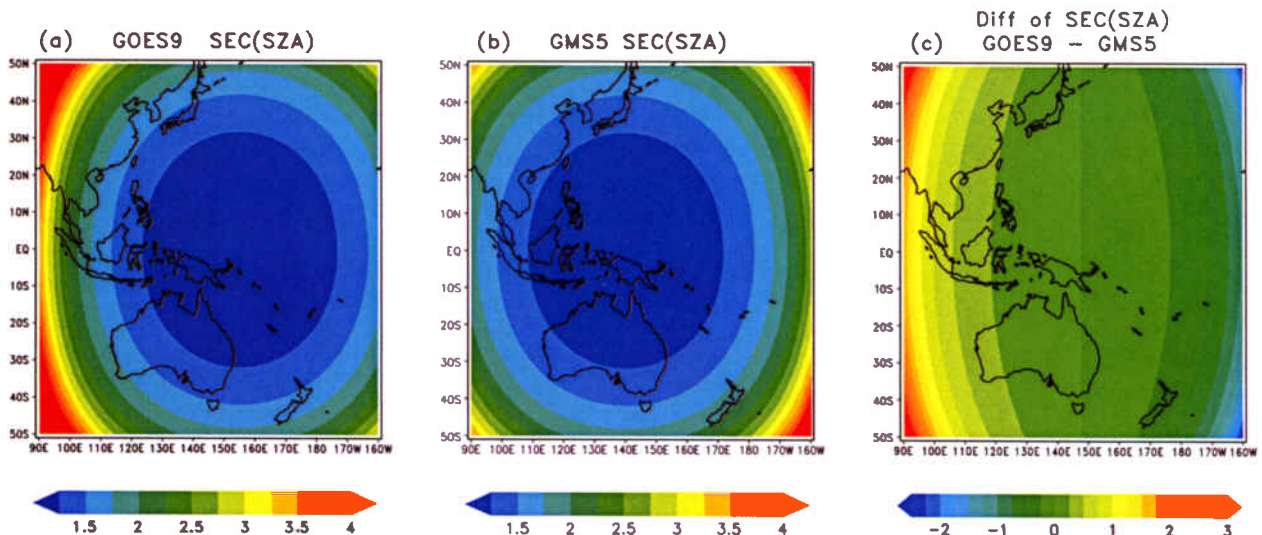


Figure 5: Secants of the satellite zenith angles to GOES-9 (a) and GMS-5 (b). Figure (c) shows the difference calculated by subtracting Figure (b) from Figure (a).

Comparisons of Brightness Temperatures for IR1

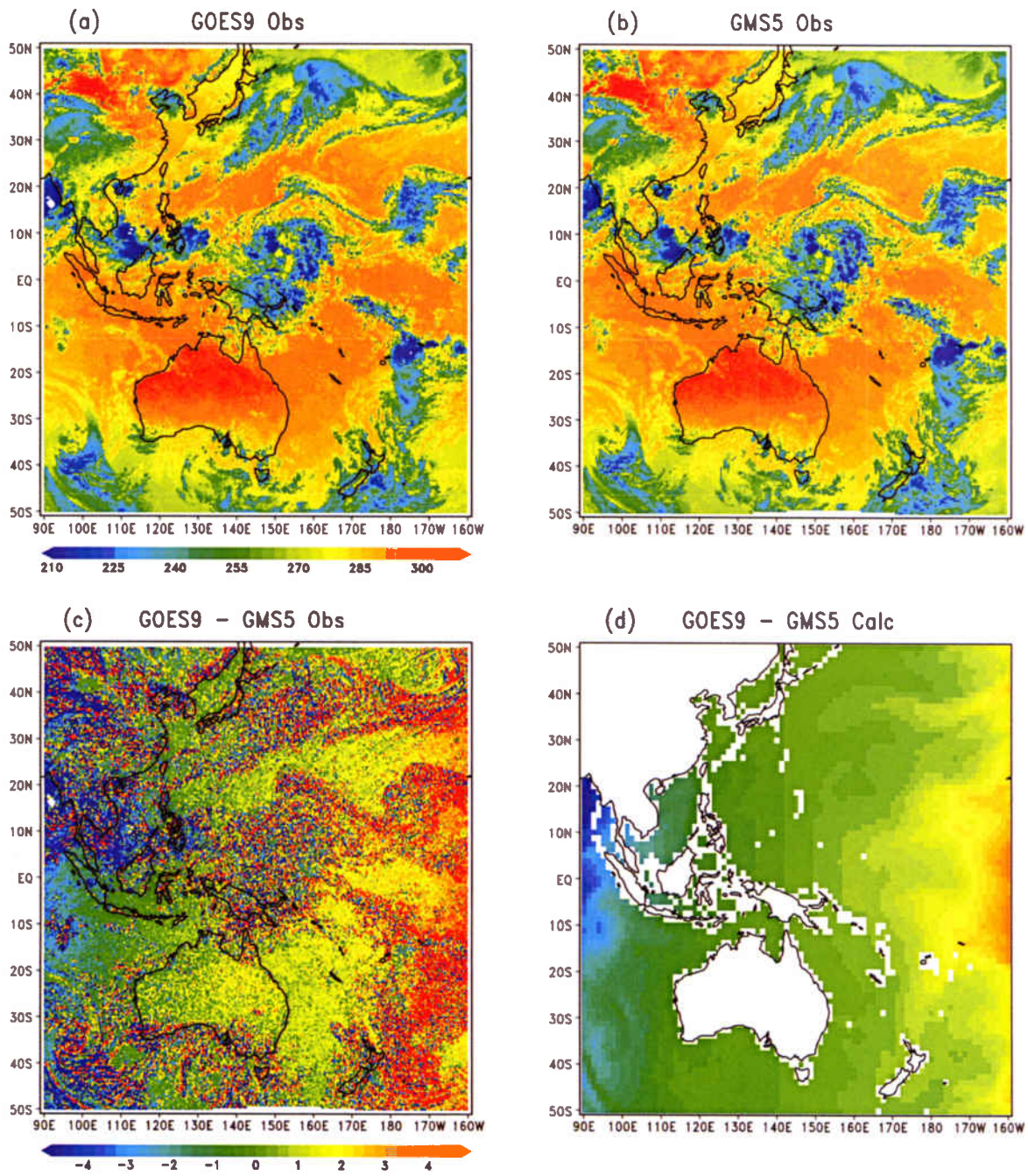


Figure 6: Images of brightness temperatures observed by GOES-9 IR1 (a) and GMS-5 (b). Figure (c) shows the difference in the observed brightness temperatures of GOES-9 from that of GMS-5. Figure (d) shows the same as Figure (c), but for the difference in the simulated brightness temperatures. The simulated temperatures are computed by MODTRAN, neglecting the atmospheric scattering effect.

Comparisons of Brightness Temperatures for IR2

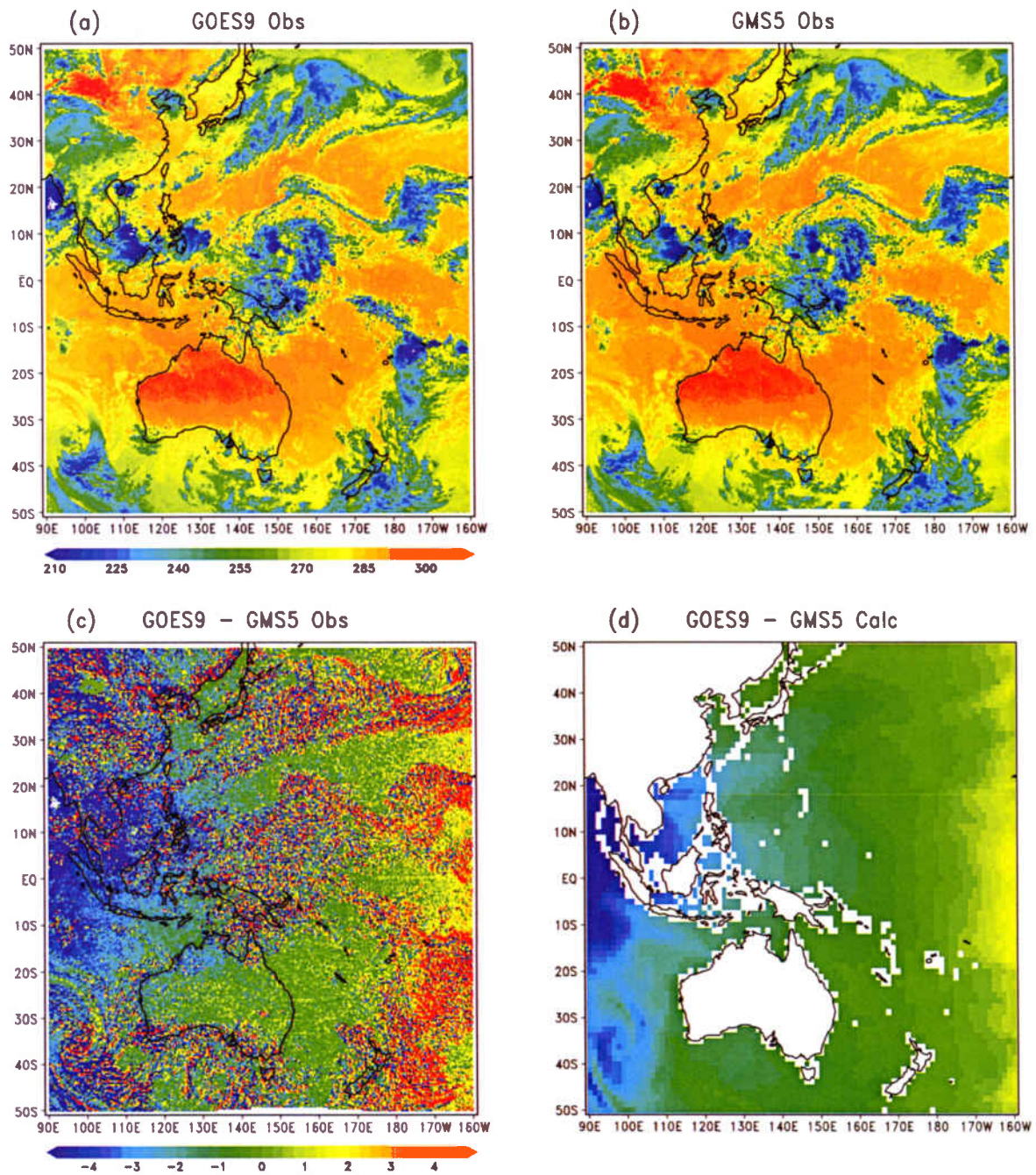


Figure 7: Same as Fig. 6, but the comparisons of IR2 images.

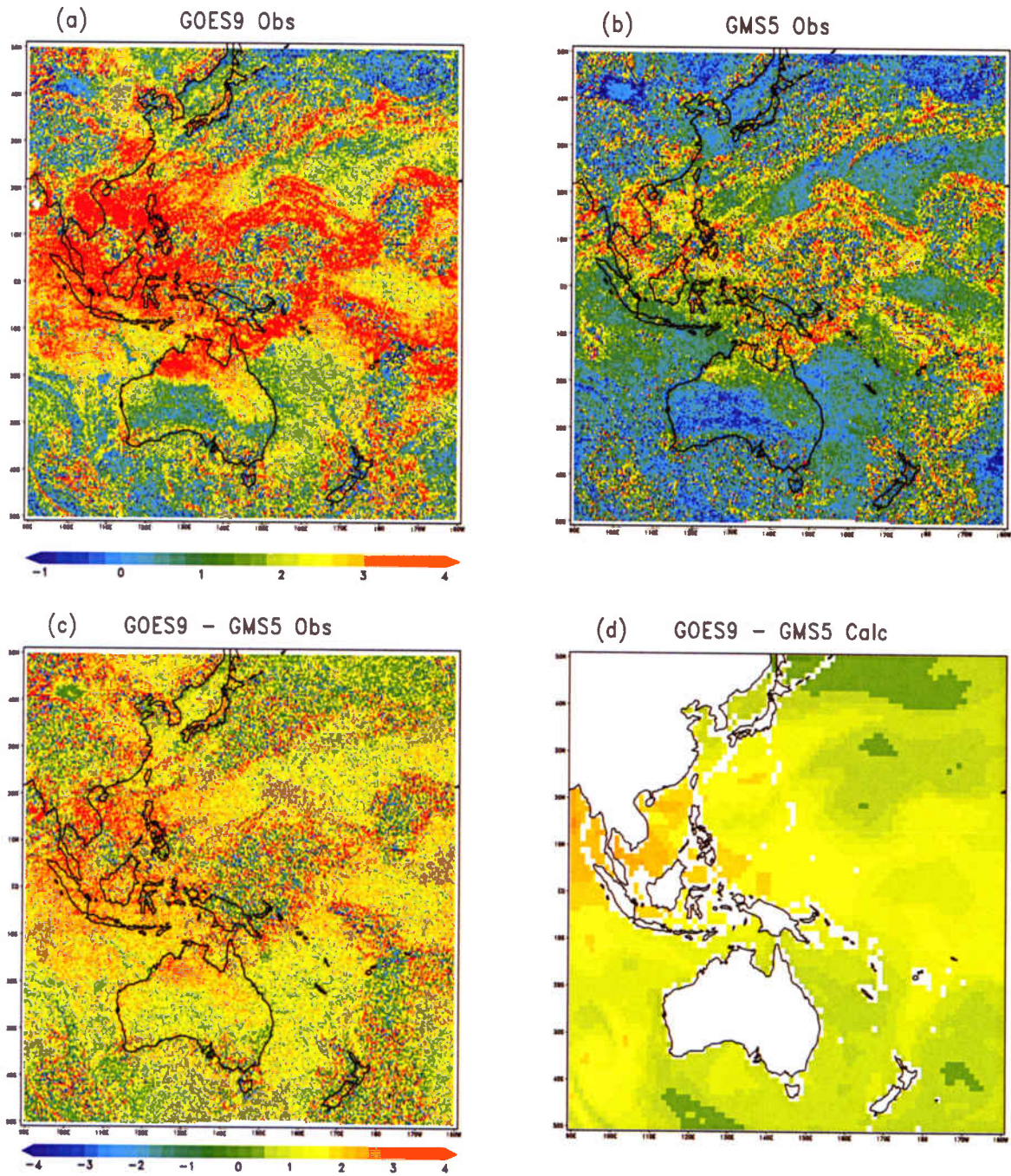


Figure 8: Same as Fig. 6, but the comparisons of differences in the brightness temperatures between the split window channels, $\delta T_{\text{SW}} = T_{\text{IR1}} - T_{\text{IR2}}$.

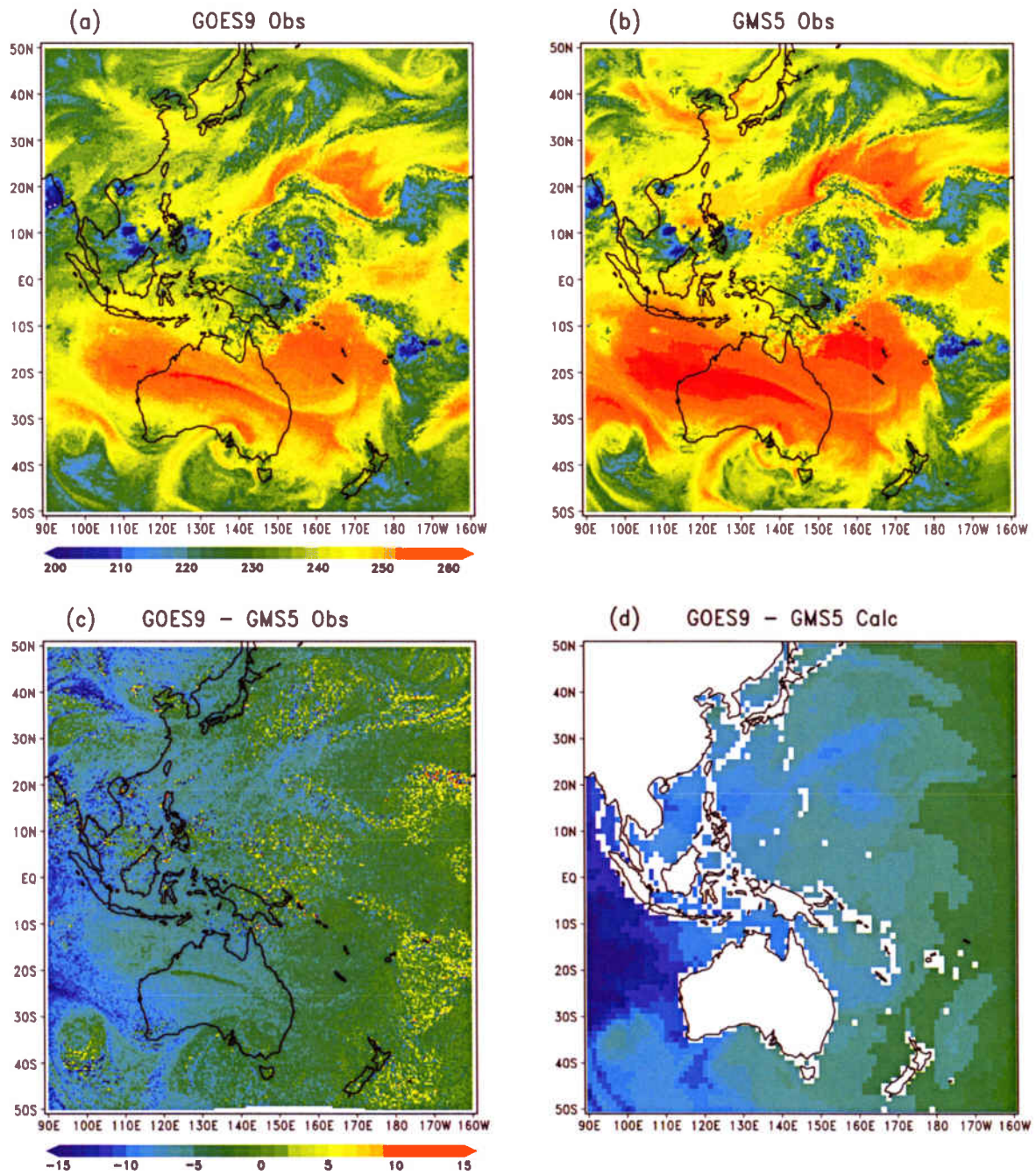


Figure 9: Same as Fig. 6, but the comparisons of WV images.

GMS5 IR1 vs. GOES9 Ch 4

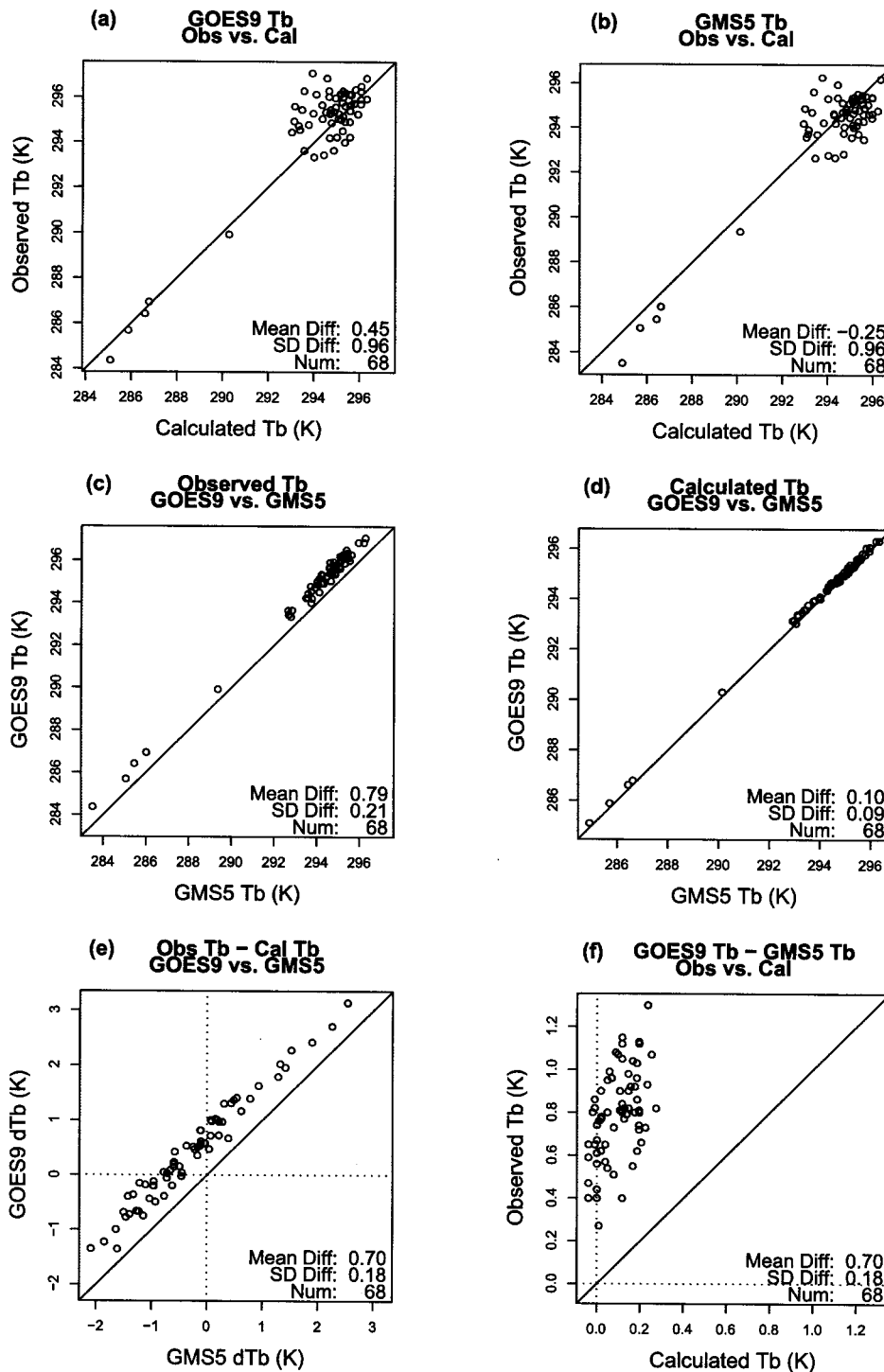


Figure 10: Comparisons of IR1 brightness temperatures; (a) GOES-9 observations versus GOES-9 simulations, (b) GMS-5 observations versus GMS-5 simulations, (c) GOES-9 observations versus GMS-5 observations, (d) GOES-9 simulations versus GMS-5 simulations, (e) observations minus simulations of GOES-9 versus those of GMS-5 and (f) GOES-9 minus GMS-5 of observations versus those of simulations. The mean difference and standard deviation between vertical elements and horizontal elements are shown as well as the number of samples.

GMS5 IR2 vs. GOES9 Ch 5

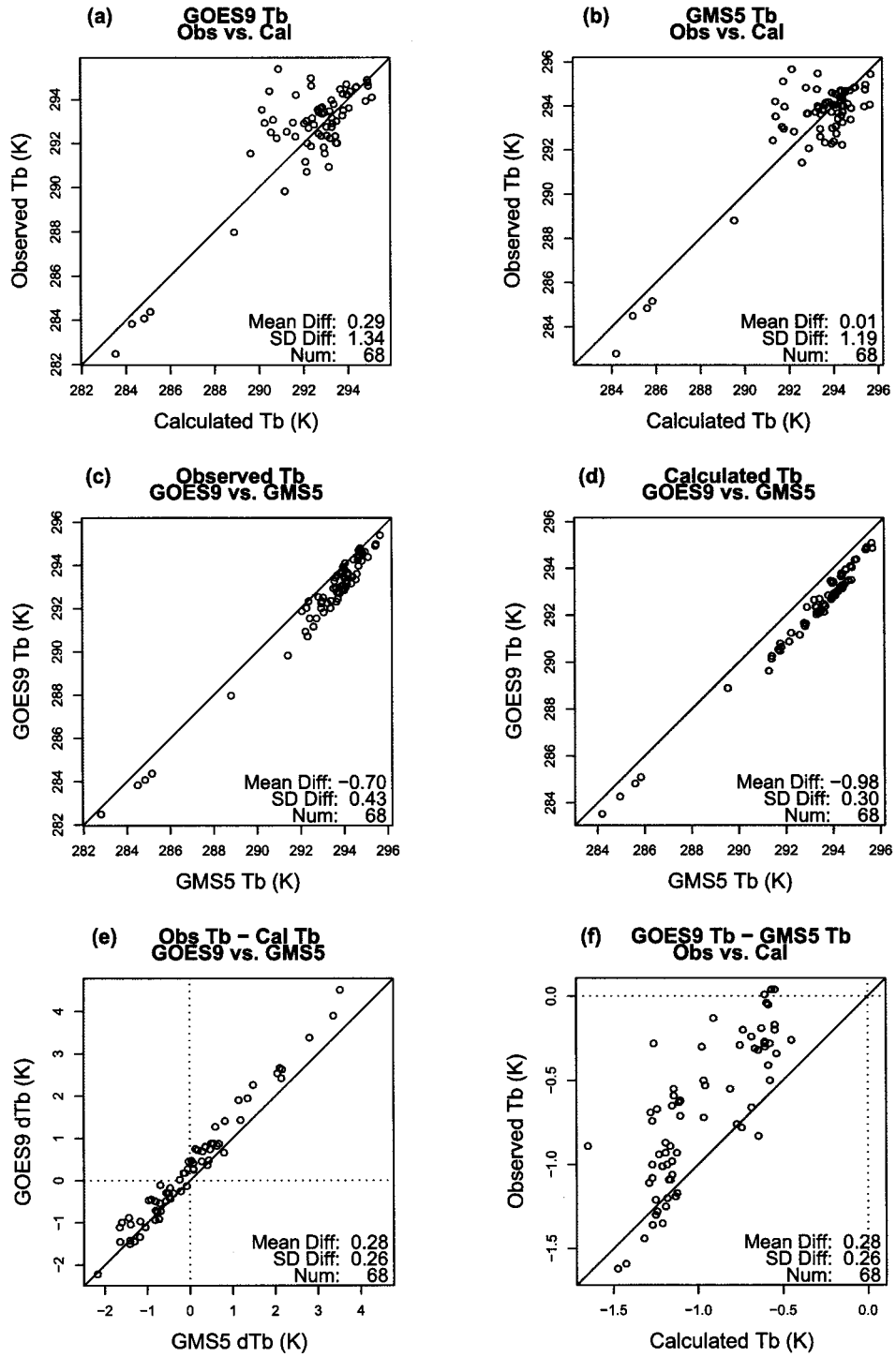


Figure 11: Same as Fig. 10, but the comparisons of IR2 brightness temperatures.

GMS5 vs. GOES9 Difference of IR1 – IR2

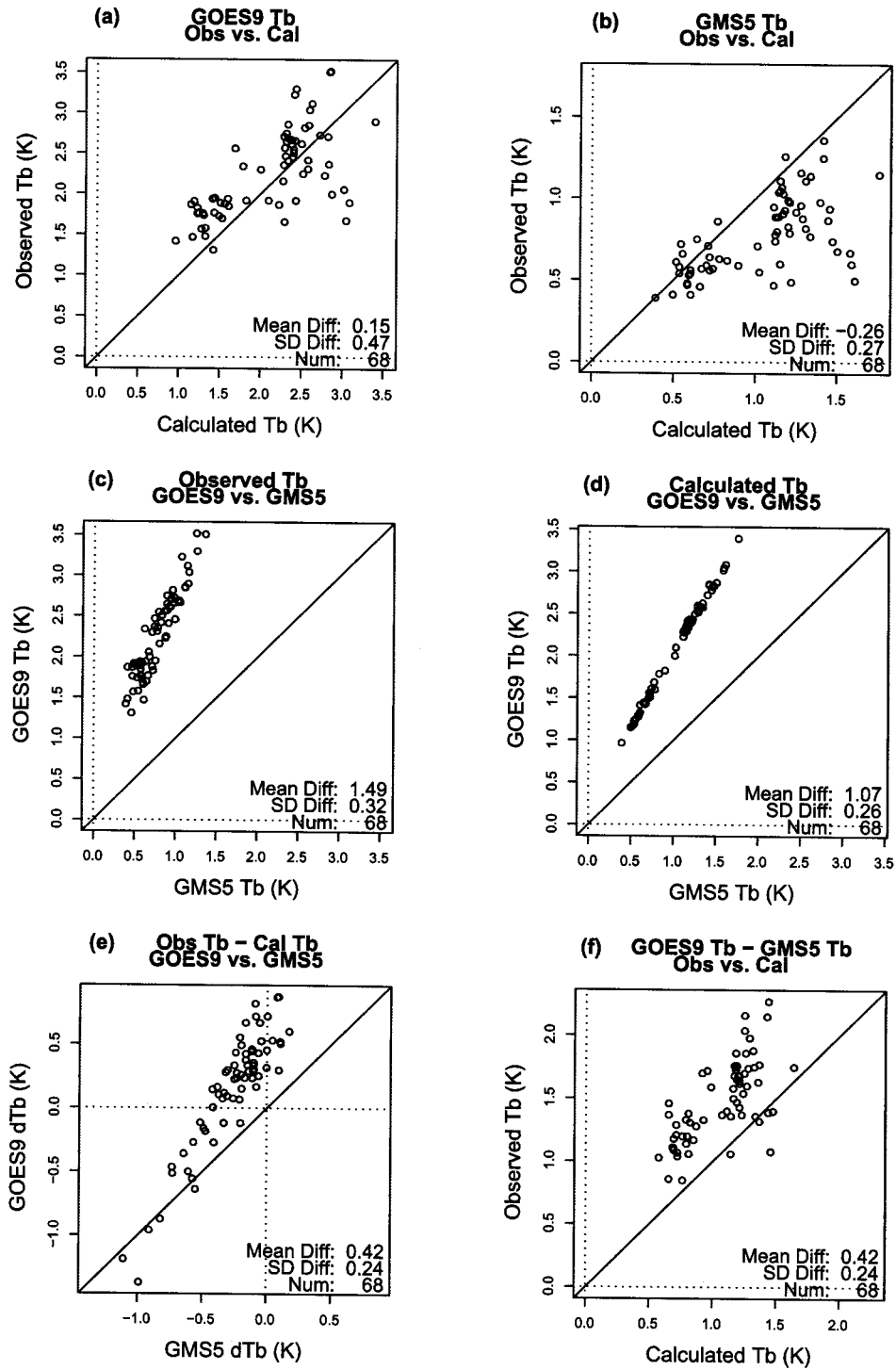


Figure 12: Same as Fig. 10, but the comparisons of differences in the brightness temperatures between the split window channels, $\delta T_{SP} = T_{IR1} - T_{IR2}$.

GMS5 WV vs. GOES9 Ch 3

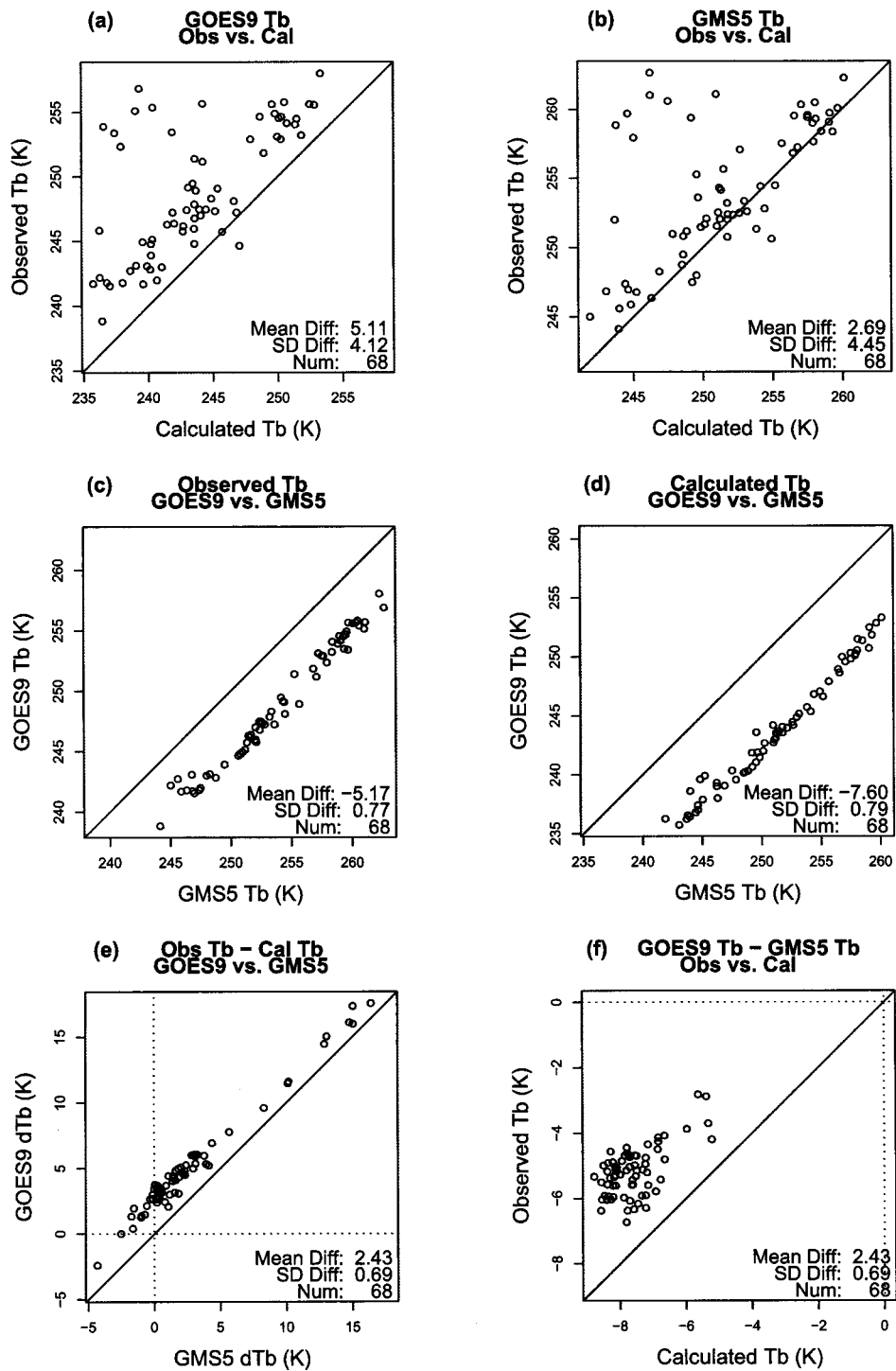


Figure 13: Same as Fig. 10, but the comparisons of WV brightness temperatures.

GMS-5およびGOES-9搭載イメージャの 赤外チャンネルインターキャリブレーション

太原 芳彦, 大河原 望, 奥山 新

気象庁 気象衛星センター
データ処理部 システム管理課

概 要

静止気象衛星による西太平洋域の観測が、2003年5月22日にGMS-5からGOES-9に切り替わった。本レポートは、各衛星に搭載されているイメージャの赤外チャンネルに関して行ったインターキャリブレーション調査結果である。

調査には、GMS-5からGOES-9への切り替え直前に得られた同時刻の観測輝度温度データを利用した。また、MODTRAN 3.7による放射計算で得られた計算輝度温度データも比較対象とした。平面図の比較からは、観測データと計算データにはほぼ同じ衛星間の差が見られ、応答関数と放射光路長に関する衛星間の違いが確認できた。さらに、雲のない海洋上で、放射光路長が2衛星間で小さい領域に関して、輝度温度データの比較統計を行った。その結果、応答関数の違いでは説明ができない衛星間の差が確認された。観測輝度温度から計算輝度温度を引いた差に関して、GOES-9とGMS-5との差を計算した結果は、赤外窓領域チャンネル1(IR1)で0.7 K、赤外窓領域チャンネル2(IR2)で0.28 K、そして水蒸気チャンネル(WV)で2.4 Kであった。この差の原因としては、キャリブレーションの誤差、センサや衛星の劣化、計算輝度温度データの誤差などが考えられるが、それを突き止めるためにはさらなる調査が必要である。原因は判っていないが、本調査による結果は、GOES-9衛星プロダクトアルゴリズムの調整に活用できる。例えば、IR1とIR2の輝度温度差に関して、GOES-9とGMS-5の間には線形関係が確認された。